Stochastic motion of solitary excitations on the classical Heisenberg chain

2000 J. Phys. A: Math. Gen. 33 2195

(http://iopscience.iop.org/0305-4470/33/11/303)

J. Phys. A: Math. Gen. **33** (2000) 2195–2207. Printed in the UK PII: S0305-4470(00)06761-5

Stochastic motion of solitary excitations on the classical Heisenberg chain

Matthias Meister and Franz G Mertens

Physikalisches Institut, Universität Bayreuth, D-95440 Bayreuth, Germany

E-mail: Matthias.Meister@theo.phy.uni-bayreuth.de and Franz.Mertens@theo.phy.uni-bayreuth.de

Received 9 August 1999, in final form January 2000

Abstract. We study stochastic motion of solitary excitations on a classical, discrete, isotropic, ferromagnetic Heisenberg spin chain with nearest-neighbour exchange interactions. Gaussian white noise is coupled to the spins in a way that allows for the noise to be interpreted as a stochastic magnetic field. The noise translates into a collective stochastic force affecting a solitary excitation as a whole. The position of a solitary excitation has to be calculated from the noisy spin configuration, i.e. the position is defined as a function of the spin components. Two examples of such definitions are given, because we want to investigate the dependence of the results on the choice of definition. Using these definitions, we calculate the variance of the position as a function of time and determine the variance from simulations as well. The calculations require knowledge of the shape of the solitary wave. We approximate the shape with that of soliton solutions of the continuum Heisenberg chain, restricting our considerations to solitary waves of large width, in which case this approximation is good. The calculations yield a linear dependence of the variance on time, the slope being determined by parameters describing the shape of the soliton. The two definitions of the position we use provide different results for this slope. The origin of this difference is discussed. With both definitions very good agreement is found between the results of the simulations and the corresponding theoretical results, for not too large time scales.

1. Introduction

Many equations modelling nonlinear physical systems exhibit solutions in the form of coherent excitations. At least approximately, these excitations behave rather like a particle than like a particular configuration of a field or of constituents of a discrete system. Most prominent examples are solitons, which appear as solutions of, for example, the Korteweg–de Vries equation or the sine–Gordon equation. Further nonlinear coherent excitations include vortices in (super)fluids or two-dimensional easy-plane magnets.

The particle-like behaviour of such excitations very often greatly facilitates theoretical work. In the case of a coherent excitation in a discrete system for instance, the degrees of freedom of the constituents of the system combine to form the coherent excitation, a usually large number of degrees of freedom thereby being submerged and replaced with considerably fewer 'effective' degrees of freedom, describing the particle-like dynamics of the coherent excitation. Coherence of an excitation can also be regarded as a family of constraints, reducing the number of degrees of freedom and leaving only particle-like ones, describable by 'collective' coordinates.

For physical reasons it is often desirable to include perturbations of the system studied into the equations of motion. These perturbations can, for instance, model the effect of

0305-4470/00/112195+13$30.00

influences from outside the system on an excitation of the system as described by a solution of the unperturbed equations. The particle-like character of coherent excitations is further emphasized by their stability against these perturbations, at least as long as the perturbations can be considered small. By stability we mean that, though some characteristics of the unperturbed system, like integrability for example, may be lost by introducing the perturbations, solutions to the unperturbed equations can often serve as very good approximations to the solutions of the perturbed system. Thus, while the solution representing, for instance, a soliton in an integrable system may no longer continue to be a soliton in the strict sense, when perturbations are introduced that destroy integrability, the solution may still represent an excitation of the system that propagates without changing its shape significantly, i.e. the excitation remains coherent. Due to this fact it is possible to use collective coordinates when studying effects of particular perturbations on coherent excitations. An especially important class of perturbations are stochastic perturbations, very often in the form of noise coupled to the system under study. Investigations of the effects of noise have been carried out, for example, for the sine–Gordon [2–5] and ϕ^4 [6, 7] equations or the above mentioned vortices in two-dimensional easy-plane magnets [8].

This paper shows the stochastic position shifts of solitary excitations on the classical, discrete, isotropic, ferromagnetic Heisenberg spin chain, when the spins are subject to Gaussian white noise.

In section 2 the Hamilton function and the equations of motion for the spins are introduced. We also present the soliton solutions of the continuum Heisenberg chain which will serve as approximations to the shape of the solitary wave on the discrete chain at a certain stage of the calculations. The equations of motion are extended to include damping and noise in section 3. We use Gilbert damping and couple the noise to the spins in a way that suggests an immediate physical interpretation of the noise as a magnetic field which is varying stochastically in space and time. In section 4 we give two examples (more can be thought of) of definitions of the position of the solitary excitation as a function of the spin components and calculate the variance of the position, approximatively neglecting magnons excited by the noise. Both definitions yield a linear dependence of the variance on time, but different results for the slope. This difference is discussed. The theoretical results of section 4 are then compared with spin dynamics simulations of the discrete chain in section 5. We find very good agreement for all choices of soliton parameters studied, at least as long as the observations are not extended over too large timespans. For longer times our theory fails, as the numerical results indicate a time dependence of the variance including higher than linear powers of time. In section 6 we discuss our results, in particular the appearance of higher powers of t in $\mathrm{Var}[X(t)]$. Finally, our results are summarized in section 7. Because of the stability of coherence we have discussed above, we take the liberty of using the terms soliton, solitary wave and solitary excitation synonymously throughout the following sections, see also the pertinent discussion in [1].

2. The Heisenberg chain

The classical, isotropic Heisenberg chain is described by the Hamilton function

$$H = -J \sum_{n=1}^{N-1} \vec{S}_n \cdot \vec{S}_{n+1} \tag{1}$$

which in the case $J > 0$ represents a ferromagnetic system. The index n labels the sites on the chain and N is the number of spins constituting the chain. The lattice constant has been set to unity, the dimensionless parameter J measures the coupling in units of a fixed, positive

scale J_0 and the spinlength is measured in units of a scale S_0. Thus energies are given in units of $J_0 S_0^2$, and time is measured in units of $\hbar/(J_0 S_0^2)$.

The equation of motion governing the dynamics is the Landau–Lifshitz equation, see [14],

$$\frac{\mathrm{d}}{\mathrm{d}t}\vec{S}_m = -\vec{S}_m \times \vec{B}_m. \tag{2}$$

Here $\vec{B}_m$ denotes an effective magnetic field at site m, the ith component of which reads $B_m^i = \mathrm{d}H/\mathrm{d}S_m^i$, resulting in $\vec{B}_m = -J(\vec{S}_{m-1} + \vec{S}_{m+1})$. It is understood that in the case of the left-most site $m = 1$ one has to drop the spin indexed $m - 1$ and that in the case of the right-most site $m = N$ no spin indexed $m + 1$ appears. Thus we are using free boundary conditions. In the continuum approximation [11, 14] the spins $\vec{S}_m(t)$ are replaced with $\vec{S}(r, t)$, and the equation of motion (2) reads

$$\frac{\mathrm{d}}{\mathrm{d}t}\vec{S} = J\vec{S} \times \partial_r^2 \vec{S}. \tag{3}$$

Equation (3) is known to possess soliton (in the strict sense) solutions [10–13], which, using spherical polar coordinates to describe the orientation of each spin in space, can conveniently be expressed in terms of fields $\Psi(r, t)$ and $\Phi(r, t)$, related to $\vec{S}(r, t)$ by

$$\vec{S} = (S^x, S^y, S^z) = S\left(\sqrt{1-\Psi^2}\cos(\Phi), \sqrt{1-\Psi^2}\sin(\Phi), \Psi\right). \tag{4}$$

Here Ψ is the cosine of the polar angle Θ. The soliton solutions read

$$\Psi(r, t) = 1 - A\left[\operatorname{sech}\left(\frac{r-X}{\Gamma}\right)\right]^2 \tag{5}$$

$$\Phi(r, t) = \Phi_0 + \omega t + \sqrt{\frac{2}{A} - 1}\,\frac{r-X}{\Gamma} + \arctan\left[\sqrt{\frac{A}{2-A}}\tanh\left(\frac{r-X}{\Gamma}\right)\right]. \tag{6}$$

The shape of the S^z distribution given by (5) is a localized pulse; at large distances from the soliton the spins tend to the same ground-state configuration on either side of the pulse. In this ground-state configuration all spins are parallel to each other and point in the z direction. The parameters Γ and A appearing in (5) and (6) are the width and the amplitude of the soliton, respectively. In the unperturbed system the excitation moves at constant speed, its position X at time t being

$$X(t) = X_0 + t \cdot JS\frac{2}{\Gamma}\sqrt{\frac{2}{A} - 1}. \tag{7}$$

Additionally, the projections of the spins onto the xy plane rotate, independently of the soliton position, at a frequency $\omega = 2JS/(A\Gamma^2)$. The energy of the soliton relative to the ground state is $E_{\mathrm{soliton}} = 4JS^2/\Gamma$. The solutions cited here will be used later to approximate the shape of solitary waves on a discrete chain.

3. Damping and noise

Taking into account damping and noise requires a modification of the equation of motion (2), a possible one being [9, 15, 16]

$$\frac{\mathrm{d}}{\mathrm{d}t}\vec{S}_m + \varepsilon\vec{S}_m \times \frac{\mathrm{d}}{\mathrm{d}t}\vec{S}_m = -\vec{S}_m \times [\vec{B}_m + \vec{b}_m] \tag{8}$$

which has to be interpreted as a Stratonovich stochastic differential equation. For similar approaches to the dynamics of magnetic moments see [17, 18]. The second term on the LHS

of (8) is Gilbert damping, which is isotropic as opposed to the Landau–Lifshitz damping [16]. Its magnitude is scaled by the parameter ε. On the RHS of this equation, a noise term $\vec{b}_m$ has been added to the effective magnetic field $\vec{B}_m$. The physical interpretation is that the stochastic perturbations considered in this article are local fluctuations of the effective magnetic field. This choice of coupling between spins and noise appears more natural than simply adding a stochastic term to the RHS of (2) as was done in [8]. Such an additive coupling lacks immediate physical interpretation. Moreover, the spinlength is not a conserved quantity of the corresponding equation of motion. The latter pain was cured in [8] by introducing conservation of the spinlength as a constraint, but this led to additional coupling terms between spins and noise, which had the structure of multiplicative couplings. In contrast to these disadvantages, the coupling we have chosen suggests the physical interpretation stated above and retains the spinlength as a conserved quantity of (8). Due to the vector product, the components of the spins and of the noise are coupled multiplicatively. A comparison between the additive coupling and the coupling chosen here can be found in [9] for the case of a two-dimensional system. The noise in (8) is Gaussian white noise, satisfying

$$\begin{aligned} &\langle \vec{b}_m(t) \rangle = 0 \\ &\langle b_m^i(t_1) b_n^j(t_2) \rangle = \sigma^2 \delta^{ij} \delta_{mn} \delta(t_1 - t_2) \\ &\sigma^2 = \mathrm{Var}(b_m^i). \end{aligned} \tag{9}$$

Together, the damping and the noise simulate the coupling of the spin chain to a thermal bath, the noise representing energy transferred to the chain from the bath, whereas the damping dissipates energy. This coupling is comparatively simple. An investigation of more complicated spin-environment couplings can be found in [19], see also references therein. The effects of damping on solitons in the continuum chain were studied in [20]. After a period of time that, as we have observed in numerical simulations, is approximately given by $5\varepsilon^{-1}$ (in dimensionless units), the mean thermal energy of the chain has reached saturation, i.e. in the mean the amount of energy supplied to the chain by the noise is equivalent to the amount of energy dissipated by the damping. For temperatures such that $k_B T / J S^2 \ll 1$ (k_B is Boltzmann's constant), the mean thermal energy per pair of neighbouring spins (there are $N - 1$ such pairs for a chain of N spins) is $k_B T$ and the variance of the noise corresponding to this saturation value is approximately $\sigma^2 = 2\varepsilon k_B T$.

4. Calculation of the variance of $X(t)$

In this section we calculate the variance of the trajectories of a solitary wave subject to noise characterized by (9). To this end, we need an expression for the position X of the excitation on the chain. We have generated numerically the time evolution of the discrete chain, using continuum soliton solutions as initial conditions; we have found that the shape of large-width solitary excitations of the discrete chain, to which our considerations are restricted, is very accurately given by the continuum soliton solutions (5) and (6). Thus we can conclude that $S - S^z$ is a symmetric pulse centred at the position of the soliton. Consequently, the first moment of this function reproduces the position of the soliton. However, this is not the only possible definition. $(S^x)^2 + (S^y)^2 = S^2 - (S^z)^2$ is also shaped like a symmetric pulse and is also centred at the soliton position. The first moment of this function thus reproduces the position of the solitary wave, as well. Of course, further suitable definitions of the position can be devised. In the following, the two examples provided above will be used.

Definition 1. *X defined as the first moment of $S - S^z$*

$$X := \frac{\sum_{n=1}^{N} n(S - S_n^z)}{\sum_{m=1}^{N}(S - S_m^z)}. \tag{10}$$

This leads immediately to

$$\frac{\mathrm{d}X}{\mathrm{d}t} = \frac{1}{\sum_{m=1}^{N}(S - S_m^z)} \sum_{n=1}^{N}(X - n)\dot{S}_n^z. \tag{11}$$

Neglecting the damping term in (8), we have

$$\frac{\mathrm{d}X}{\mathrm{d}t} = \frac{\sum_{n=1}^{N}(X - n)[-\vec{S}_n \times \vec{B}_n]_z}{\sum_{m=1}^{N}(S - S_m^z)} + \frac{\sum_{n=1}^{N}(X - n)[-\vec{S}_n \times \vec{b}_n]_z}{\sum_{m=1}^{N}(S - S_m^z)}. \tag{12}$$

Now we approximate the vectors $\vec{S}_n$ with their 'deterministic' values, i.e. we regard $\vec{S}_n$ as given by the fictitious spin configuration obtained when neglecting magnons excited by noise but keeping the noise-induced stochastic nature of X. Note that both fractions in (12) contain X. However, X only appears in the combination $(X - n)$, so that sums containing this expression can be considered as sums over indices relative to the current position of the soliton. Thus, these sums are independent of the position of the soliton, at least approximately. A dependence on the exact position of the solitary wave cannot be ruled out entirely, because X takes values in the reals, whereas n is limited to integer values. As we consider only excitations of a width much larger than the lattice constant, this dependence should be very weak and henceforth we shall neglect it. Then (12) can be written

$$\frac{\mathrm{d}X}{\mathrm{d}t} = F_{\mathrm{det}} + F_{\mathrm{st}}(t) \tag{13}$$

with a deterministic and a stochastic part of the force. Here the two terms on the RHS are defined by the corresponding two fractions on the RHS of (12). Within the above approximations the deterministic part of the force is constant and the time dependence of the stochastic part is caused only by the time dependence of the noise. We therefore split $X(t) = X_{\mathrm{det}}(t) + X_{\mathrm{st}}(t)$, where X_{det} and X_{st} are defined as solutions to

$$\frac{\mathrm{d}X_{\mathrm{det}}}{\mathrm{d}t} = F_{\mathrm{det}} \tag{14a}$$

$$\frac{\mathrm{d}X_{\mathrm{st}}}{\mathrm{d}t} = F_{\mathrm{st}}(t) \tag{14b}$$

respectively. Equation (14*b*) with the initial condition $X_{\mathrm{st}}(0) = 0$ yields

$$X_{\mathrm{st}}(t) = \int_0^t F_{\mathrm{st}}(t')\mathrm{d}t'. \tag{15}$$

Thus

$$\langle X_{\mathrm{st}}(t_1)X_{\mathrm{st}}(t_2)\rangle = \int_0^{t_1}\int_0^{t_2}\langle F_{\mathrm{st}}(t_1')F_{\mathrm{st}}(t_2')\rangle \mathrm{d}t_1'\,\mathrm{d}t_2'. \tag{16}$$

Using the explicit form of F_{st} and the properties of the noise, (9), we get

$$\langle F_{\mathrm{st}}(t_1')F_{\mathrm{st}}(t_2')\rangle = \sigma^2 \frac{\langle\sum_{n=1}^{N}(X - n)^2[S^2 - (S_n^z)^2]\rangle}{[\sum_{m=1}^{N}(S - S_m^z)]^2}\delta(t_1' - t_2'). \tag{17}$$

In the derivation of (17) we had to calculate expressions such as

$$\left\langle \sum_{n,m}(X(t_1') - n)(X(t_2') - m)S_n^x(t_1')S_m^x(t_2')b_n^y(t_1')b_m^y(t_2') \right\rangle \tag{18}$$

which were evaluated to

$$\sum_{n,m}\langle (X(t_1')-n)(X(t_2')-m)S_n^x(t_1')S_m^x(t_2')\rangle\langle b_n^y(t_1')b_m^y(t_2')\rangle \tag{19}$$

likewise for similar expressions. This would be correct if noise and spin configuration were completely uncorrelated. We have already approximated the spin configuration by neglecting magnons, so the only remaining correlation between spins and noise must stem from the influence the noise has on X. As the spin components in (18) are themselves functions of $X-n$, shifts of X can only change the sum due to differences between the noise components in the vicinity of the shifted and the unshifted position. The components of the noise are, however, mutually uncorrelated. Therefore the replacement (18) $\rightarrow$ (19) appears justified. Another way of seeing this is the following: (14*b*) has to be interpreted as a Stratonovich stochastic differential equation for the variable X_{st}; it can be transformed to Ito form [21]. No additional deterministic contributions arise from the transformation in this case. The noise components and the stochastic variable X_{st} are rendered uncorrelated, however. So the above replacement is exact within the 'deterministic' approximation for the spins $\vec{S}_n$ introduced after (12). The problem of correlations between spins and noise was similarly addressed in [9].

To explicitly evaluate (17) we now make use of the soliton solution for the continuum, (5). Replacing $X-n \rightarrow X-r$ we find

$$\langle F_{\mathrm{st}}(t_1')F_{\mathrm{st}}(t_2')\rangle = \sigma^2\frac{\int (r-X)^2[1-\Psi^2]\mathrm{d}r}{[\int(1-\Psi)\mathrm{d}r]^2}\delta(t_1'-t_2'). \tag{20}$$

Using (5) and (20) in (16) leads to

$$\langle X_{\mathrm{st}}(t_1)X_{\mathrm{st}}(t_2)\rangle = \frac{\sigma^2}{36}\Gamma\left[\frac{3\pi^2}{A}+6-\pi^2\right]\min(t_1,t_2). \tag{21}$$

As we are especially interested in the variance of the trajectory and use noise with $\sigma^2 = 2\varepsilon k_B T$, we can write:

$$\mathrm{Var}[X(t)] = \mathrm{Var}[X_{\mathrm{st}}(t)] = \frac{\varepsilon k_B T\Gamma}{18}\left(\frac{3\pi^2}{A}+6-\pi^2\right)t. \tag{22}$$

Definition 2. *X defined as the first moment of $(S^x)^2+(S^y)^2$.*

Here we define X as

$$X := \frac{\sum_n n[(S_n^x)^2+(S_n^y)^2]}{\sum_m[(S_m^x)^2+(S_m^y)^2]}. \tag{23}$$

Taking the time derivative on both sides results in

$$\dot{X} = \frac{2}{\sum_m[(S^x)^2+(S^y)^2]}\sum_n (n-X)(S_n^x\dot{S}_n^x + S_n^y\dot{S}_n^y). \tag{24}$$

Proceeding with this equation in the same way as with the corresponding equation in the case of the first definition of X, (10), one obtains a stochastic force

$$F_{\mathrm{st}} = -\frac{2}{\sum_m[(S_m^x)^2+(S_m^y)^2]}\sum_n (n-X)[S_n^x(S_n^y b_n^z - S_n^z b_n^y) + S_n^y(S_n^z b_n^x - S_n^x b_n^z)]. \tag{25}$$

The correlation function of the stochastic force in continuum approximation is

$$\langle F_{\mathrm{st}}(t_1)F_{\mathrm{st}}(t_2)\rangle = \frac{4\sigma^2\delta(t_1-t_2)}{\int(1-\Psi^2)\,\mathrm{d}r}\int (r-X)^2\Psi^2(1-\Psi^2)\,\mathrm{d}r \tag{26}$$

and we finally arrive at

$$\mathrm{Var}[X(t)] = \frac{\varepsilon k_B T \Gamma}{70(A-3)^2}\left[1050 + 196A^2 - 840A + \pi^2\left(112A - 175 - 24A^2 + \frac{105}{A}\right)\right]t. \tag{27}$$

Obviously the results (22) and (27) are different and will be discussed below. With both definitions of the soliton position the resulting expression for the variance is independent of J and S. The linear dependence on t shows that the stochastic motion of the soliton is a simple random walk, with an effective diffusion constant D—defined as the slope of $\mathrm{Var}[X(t)]$ as a function of time. D depends on the shape of the soliton, which is parametrized by Γ and A. The linear dependence on Γ is no surprise. The stochastic forces F_{st}, (12) and (25), are given as sums over lattice sites, to which only sites near the soliton contribute essentially. Within the approximations detailed above, the contributions of individual sites are mutually stochastically independent. So the variance of the sum of these contributions equals the sum of the variances of the contributions of all individual sites. The number of sites contributing essentially to this sum should be proportional to the width Γ of the soliton. Additional factors appearing in (22) and (27), apart from damping, temperature and time, take into account that the contributions from different sites are not equal, but are weighted by the structure of the soliton.

For both definitions of X the spin configuration has been approximated with the unperturbed soliton structure. Thus at first sight it may appear strange that the results are different. To understand this difference it is necessary to realize how the noise actually effects a shift of the soliton position. The noise creates fluctuations of the spin configuration. In turn, these fluctuations result in distortions of the respective weights, $S - S^z$ for the first definition and $(S^x)^2 + (S^y)^2$ for the second definition. Upon evaluation of (10) or (23), these distortions generate shifts of X. As can be seen from (10) and (23), only that part of a distortion of a weight function which is antisymmetric with respect to the current value of X can shift X. The approximation we have made when replacing the spin configuration with the unperturbed one consists in putting an unperturbed soliton at this shifted position and neglecting any fluctuations still remaining. As details of the fluctuations are different between the two weights used, shifts of X induced by the fluctuations are different. This explains the difference in the results. We stress that the significant dependence of the effective diffusion constant on the definition of the position is most likely not a peculiarity of the solitons studied in this article. On the contrary, it has to be taken into account for all investigations of like kind.

Concluding this section we mention that by treating the sums in the deterministic part of the force in a similar way as detailed above for the stochastic forces, both definitions of the position X yield

$$\frac{\mathrm{d}X_{\mathrm{det}}}{\mathrm{d}t} = JS\frac{2}{\Gamma}\sqrt{\frac{2}{A} - 1}. \tag{28}$$

This result agrees with (7).

5. Results from simulations

We have performed simulations for the discrete chain, numerically solving (8) by means of the Heun algorithm, which is particularly suited for the Stratonovich treatment of multiplicatively coupled stochastic terms [22]. The simulations have been done for different temperatures and a variety of soliton parameters A and Γ. Soliton solutions of the continuum equation have served as initial configurations. As stated above, this approximation to solitary waves on the discrete chain is justified, provided the width is large compared with the lattice constant. The

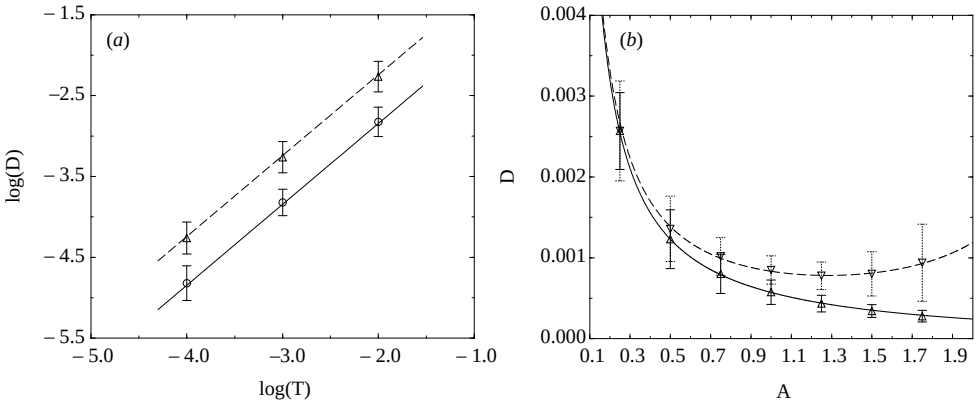

Figure 1. Slope D of Var$[X(t)]$. Symbols represent least square fits to numerical results obtained from 1000 realizations of 25 time unit runs. Error bars give one standard deviation. $J = 1$, $S = 1$. (*a*) Results from definition 1 for $T = 0.0001$, 0.001, 0.01 and $A = 1$. ○: $\Gamma = 10$, $E_{\text{soliton}} = 0.4$, the prediction is shown as a solid line; △: $\Gamma = 40$, $E_{\text{soliton}} = 0.1$, the prediction is given as a dashed line. The threshold is 0.1. (*b*) Results for $T = 0.001$, $\Gamma = 40$. D as function of A. Comparison between definition 1 (△), prediction plotted as a solid curve and definition 2 (▽), prediction given as a dashed curve. The threshold is 0.01.

latter is equal to 1 in our case and the smallest value chosen for the width in the simulations is $\Gamma = 10$. For both weights, $S - S^z$ and $(S^x)^2 + (S^y)^2$, only sites where the weight function is larger than a certain threshold are taken into account when the soliton position is calculated from the spin configuration. At these sites the value of the weight function is reduced by the threshold value. This procedure excludes contributions of those fluctuations from the sums in (10) and (23) which are located at a distance from the soliton. Inclusion of such fluctuations obviously would be erroneous. The reduction of the weight function by the threshold value reduces some errors caused by the discreteness of the system. Strictly speaking the threshold should be taken into account in the theoretical prediction. The integrals (20) and (26) should be restricted to those intervals where the weight functions are above the threshold. However, the thresholds used are small in comparison with the amplitudes of the weight functions and therefore this correction has been neglected. The damping parameter is $\varepsilon = 0.01$ in all cases. The variance of the noise is $2\varepsilon k_B T$ where T is the temperature the system would assume in saturation. Of course this statement is only valid as long as $k_B T/(JS^2) \ll 1$, see section 3. In the captions T denotes $k_B T$ in units of $J_0 S_0^2$.

Figure 1 shows some results obtained by measuring the variance of the position from simulations and least square fitting a straight line $v(t) = Dt$ to these numerical results. The slopes D so determined are given as symbols in the figure. The error bars give one standard deviation of the numerical data points from the fitted straight line. Note that the results in the figures represent the 'short-time' behaviour of the corresponding excitations, as the numerical results have been taken from runs of 25 time units. Figure 1(*a*) shows the T-dependence at fixed amplitude A for two values of the width; in both cases there is very good agreement between theory and simulation. Figure 1(*b*) provides data for fixed width, fixed temperature and various values of A, comparing the results for the two definitions of the position. Very good agreement between theory and simulations is found for both definitions. Thus the dependence of D on the definition for the position, derived analytically in the previous section, is seen to be confirmed by simulations. This is especially obvious for the data points belonging to larger values of A.

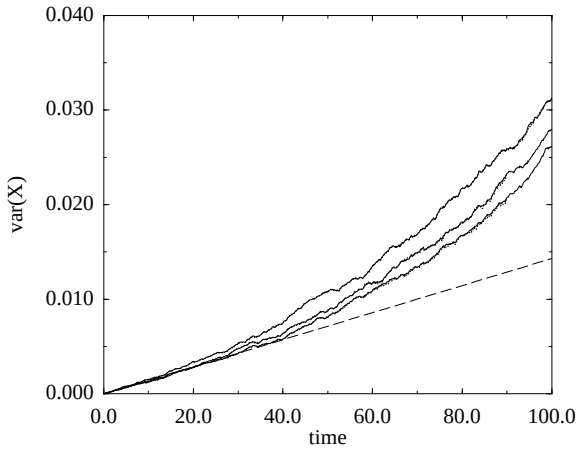

Figure 2. Variance of X as a function of time, determined with definition 1. Soliton parameters: $A = 1$, $\Gamma = 10$. $T = 0.001$. 500 realizations. Solid curve: $S = 1$, $J = 1$, dotted curve: $S = 2$, $J = 0.5$. In order of increasing deviation from the prediction (dashed curve) the graphs correspond to threshold values of 0.05, 0.1, 0.2 for $S = 1$ and to threshold values of 0.1, 0.2, 0.4 for $S = 2$.

It has just been shown that the short-time behaviour of a solitary excitation is described well by the results of the previous section. For longer times, deviations between theory and simulations like those shown in figure 2 occur. Var$[X(t)]$ as a function of t involves higher than linear powers of t. The time interval after which this deviation from the linear dependence on time becomes obvious depends significantly on the width of the excitation; the dependence on A is less important, as long as A is considerably larger than the amplitudes of the thermal excitations. For $\Gamma = 10$, as in figure 2, this time is about 25 time units, for $\Gamma = 20$ about 50 time units and for $\Gamma = 40$ the linear dependence is confirmed up to about 630 time units. These deviations can be expected to occur sooner or later *for all choices* of the parameters Γ and A.

Before we conclude this section we turn shortly to the saturated case. A length of time equal to about 500 time units has been found sufficient for taking the system into energetic saturation—understood of course as a statement referring to the average over a large number of realizations. We have generated a 'saturated' configuration by performing a 500 time unit prerun with one realization and then have used this configuration as the initial configuration for runs over 4000 realizations from which the positions and the variance of the positions have been determined. The results are shown in figure 3. The situation is basically the same as for the unsaturated case discussed above. The short-time behaviour is well described by the formulae derived in section 4. Higher than linear powers of t appear after about 20 time units for the soliton of width $\Gamma = 10$, while for the excitation with $\Gamma = 40$ the linear behaviour is confirmed for longer times—we have restricted the simulations to 100 time units to save computing time. In the saturated case magnons abound on the chain, but at least for the temperature range investigated here, they do not have any significant effect on the (initial) slope of Var$[X(t)]$. The predictions shown in the graphs correspond to the calculations of section 4, in which thermally excited magnons have been neglected. We therefore conclude that apart from the appearance of higher powers of t in the behaviour of Var$[X(t)]$, which also show up in the unsaturated case, the theory developed in section 4 can be applied to the saturated case as well. Our further investigations therefore focus on the unsaturated case. As the higher powers of t seem to appear in Var$[X(t)]$ for all excitations and to have a common

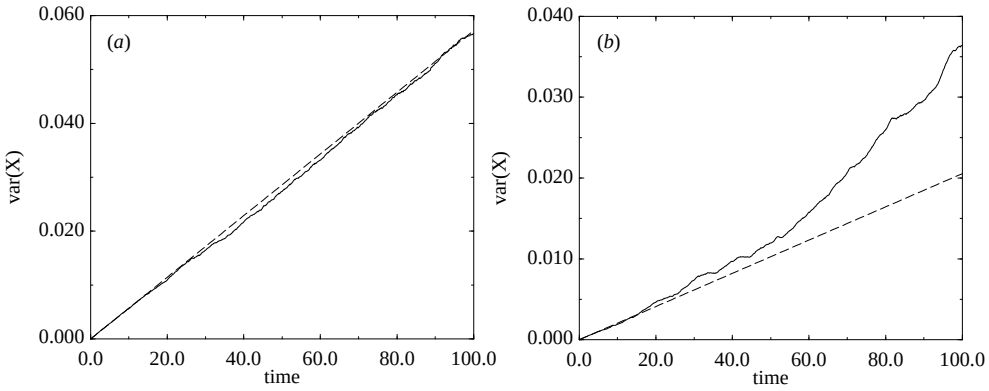

Figure 3. Results in saturation after a prerun of 500 time units. $T = 0.001$. $J = 1$, $S = 1$. Dashed line: theory, solid curve: numerical results (average over 4000 realizations, definition 1, threshold 0.1). (*a*) Before the prerun the soliton parameters were $A = 1$, $\Gamma = 40$, $E_{\text{soliton}} = 0.1$. The effects of damping were small during the prerun, thus those parameters have been used for the prediction. (*b*) Before the prerun the soliton parameters were $A = 1$, $\Gamma = 10$. For this excitation the effects of the damping were larger. The parameters used in the prediction have been obtained as $\Gamma = 11.3$, $A = 0.8$ by fitting the continuum solution to a configuration obtained from a 500 time unit run with damping, but without noise. $E_{\text{soliton}} \approx 0.354$.

cause, we study their behaviour in the case of the soliton of width $\Gamma = 10$ and $A = 1$, where the higher powers of t can be observed rather early, to reduce computing time.

6. Discussion

For sufficiently long times $\mathrm{Var}[X(t)]$ deviates from the predicted linear dependence on t. In the derivation of the theoretical results we have neglected damping. Therefore, we have checked if this approximation is the reason for the deviations. We have performed a simulation for soliton parameters $\Gamma = 10$ and $A = 1$, with no damping, i.e. $\varepsilon = 0$, but a variance of noise equal to that obtained for $\varepsilon = 0.01$, i.e. $\sigma^2 = 2 \times 0.01 \times k_B T$. The resulting graph for $\mathrm{Var}[X(t)]$, which has not been included in this paper, up to tiny fluctuations, is identical to the corresponding graph obtained with damping and in particular it exhibits the same deviations from theory.

Furthermore, the magnitude of the deviation depends significantly on the threshold introduced in section 5. Numerical results with different thresholds but A, Γ, T fixed are shown in figure 2 for two spinlengths S. All graphs relating to the same S have been obtained from identical spin dynamics, the only difference between the graphs being the threshold values. Considering the deviation as a function of the threshold value and extrapolating this to threshold zero yields a smaller, but still non-zero deviation.

The theoretical predictions for $\mathrm{Var}[X(t)]$, (22) and (27), are independent of the coupling J and the spinlength S. The general observation is that the deviations increase (decrease) with increasing (decreasing) JS. In figure 2, J and S are varied in such a way that JS remains constant. Scaling the threshold with the spinlength results in practically identical deviations, for instance the deviation is the same for $J = 1$, $S = 1$, threshold value 0.1 and for $J = 0.5$, $S = 2$, threshold value 0.2. Note that the initial slopes of all graphs shown in figure 2 agree with each other and with the theoretical prediction. As we have already pointed out in section 4, we neglect noise-induced magnons in our theoretical calculations. Thus, we think that the observed deviations from theory are caused by these fluctuations. An investigation of the

dynamical effects of magnons, for instance along the lines exposed in [7] for the ϕ^4 and in [5] for the sine–Gordon system, requires careful attention to the different behaviour of magnons in a continuum and a discrete system; for instance differences occur in the magnon dispersion relation and the soliton–magnon interaction. Though definitely interesting, this investigation is beyond the scope of the present paper. While the magnons will surely influence the dynamics, they may also lead to errors in the determination of the soliton position which result from the fact that under noise one never observes the pure soliton structure on the chain, but always the soliton in the midst of interaction with thermal excitations. Below we discuss the latter effects. The discreteness of the system can amplify these effects of the magnons: when determining the soliton position as first moment of one of the weight functions (10) and (23), only sites where the value of the weight function exceedes a threshold are taken into account. Consider now for instance a site where the unperturbed weight function would be only slightly higher than the threshold. At this site even a very small fluctuation can reduce the weight function to a value below the threshold, so the site no longer contributes to the sums in formulae (10) and (23). A site of the discrete model corresponds to a part of the continuum chain which has a spatial extent of one lattice constant. In the continuum, however, a fluctuation at a point where the weight function is slightly above the threshold need not cut an area of a width of one lattice constant from the integrals replacing the sums in (10) and (23). The region cut out may be far smaller, if the fluctuation is sufficiently localized; not so for the discrete chain. For broader excitations this effect is suppressed, as a broader excitation encompasses a larger number of sites where the weight function is well above the threshold. Raising the threshold for a given excitation leaves a smaller part of the soliton to be taken into account in the determination of X, in particular a lower number of sites. Thus the weight of an error, caused by discreteness or otherwise, usually increases in comparison to the part of the weight function still above the threshold. As the excitations have finite size, deviations do not disappear when extrapolated to threshold zero, but assume a minimum non-zero magnitude corresponding to a minimum relative weight of a given error.

Increasing JS causes both fluctuations and the soliton to travel faster along the chain and so more magnons per time unit will interact with the soliton and pass those sites where the unperturbed weight function is close to the threshold. Therefore, the determination of X will pick up more errors and the deviations increase. Lowering JS reduces the speed of fluctuations and solitons, consistently resulting in reduced deviations.

Varying J and S with JS fixed keeps all speeds constant. If, for any given spin configuration, the threshold is scaled with the spinlength, the weight function $S-S^z$ will always be above or below the threshold value at exactly the same sites. Thus the sites contributing to the sums in (10) will also be the same. If a part of the spin configuration is excluded from these sums because of the discreteness of the system, as described above, the magnitude of the resulting error in each of the sums will scale with the spinlength, because the weight function scales with S. Any errors due to neglected distortions of the part of the weight function above the threshold should scale with S as well, at least approximately. These factors, however, will mutually cancel between numerator and denominator of the fraction defining X, (10). Thus the net error will be the same for different spinlengths. This explains the scaling of the deviations shown in figure 2.

Finally we want to discuss the meaning of the differing results derived in section 4 and confirmed by simulations in section 5. The disagreement between the results for the two definitions used as examples in this paper has been explained with the different way a given deformation of the spin configuration is translated into a position shift by each weight function. However, as the soliton itself, the weight functions are localized. Therefore, one can expect that there is an upper limit for the magnitude of the position shifts, above which these differences

are no longer dominant. Consider for example several realizations for a soliton of given width Γ. Assume that the positions of the soliton differ between the realizations by several 100 widths on the average. Then the variance of the position is dominated by this large average separation, and not by the different answers from different ways of evaluating the position, because these differences obviously are restricted to an order of magnitude comparable to the width of the excitation.

We think that none of our results can be reckoned to belong to this long-time regime. Especially, the deviations observed cannot be considered as the onset of a cross-over behaviour, because for this they show much too early, at standard deviations of the position corresponding to about 0.006 times the width ($\Gamma = 10$, $A = 1$, $T = 0.001$, $t = 25$); furthermore, for given soliton parameters the deviations occurring for both definitions of the position show no signs of asymptotically approaching a common value.

The long-time regime where the differences between the definitions are suppressed can probably not be reached at all. In order to achieve sufficiently large standard deviations, one would have to consider very long times, during which, however, the damping changes the soliton parameters significantly. In particular the width increases drastically; thus, while one is waiting for the standard deviation to grow large enough to be comparable to the original width of the soliton, the width itself grows strongly. Finally, the soliton is destroyed by the damping. Performing simulations without damping would lead to the soliton being completely submersed in magnons after some time, and so the soliton can no longer be detected. Moreover, the case without damping is rather unphysical, as the fluctuation-dissipation theorem is violated.

7. Summary and conclusion

We have studied the effects of noise on the trajectories of solitary excitations on a discrete Heisenberg chain. Using the first moments of the weight functions $S - S^z$ or $(S^x)^2 + (S^y)^2$ as examples of definitions of $X(t)$ we have predicted a linear dependence of $\mathrm{Var}[X(t)]$ on time. Each definition provides a different result for the slope of the pertaining graph. The difference occurs because the excitations are not rigid, but can be distorted by fluctuations. Then the corresponding distortions of each weight function shift the value of the position calculated as first moment of the respective weight function. This dependence shows that care has to be taken as to which theoretical result is to be compared with which numerical result; it must be assured that the definition used in the theory corresponds to that used in the numerical work. The need for this care is most likely not limited to the Heisenberg chain.

We have found that for not too large time scales (depending on the soliton parameters) theory and simulations are in good agreement. In this time regime and in the temperature range studied, the solitary excitations perform a random walk with an effective diffusion constant depending on the soliton parameters Γ and A and linearly on temperature. Furthermore, it has turned out that our predictions apply to energetically saturated systems also, though only noise enters the calculation while thermally excited magnons are neglected. For sufficiently long times higher powers of t appear in the behaviour of $\mathrm{Var}[X(t)]$, both for an unsaturated and a saturated system. We have related these deviations between theory and simulation to magnons neglected in the calculations. On the one hand magnons can influence the dynamics of the system, and this effect has not been studied here. On the other hand, magnons can lead to errors in the determination of the soliton position, which has been discussed, and the relevant conclusions have been supported by numerical results.

Note added in proof. Meanwhile we have found that the higher powers of t appearing in $\mathrm{Var}[X(t)]$ can be related to stochastic fluctuations of the soliton structure. These fluctuations can be captured by a different approach based on

implicit collective coordinates (see [1] for a definition of the latter). This approach reproduces the higher than linear powers of t in Var$[X(t)]$ as observed in spin dynamics simulations.

Acknowledgments

The authors acknowledge fruitful discussions with A R Bishop, G Lythe (Los Alamos), A Sanchez, E Moro, N R Quintero (Madrid) and Y Gaididei (Kiev).

References

[1] Rajaraman R 1982 *Solitons and Instantons* (Amsterdam: North-Holland)
[2] Pascual P J and Vazquez L 1985 *Phys. Rev.* B **32** 8305
[3] Biller P and Petruccione F 1990 *Phys. Rev.* B **41** 2139
[4] Petruccione F and Biller P 1990 *Phys. Rev.* B **41** 2145
[5] Quintero N R, Sanchez A and Mertens F G 1999 *Phys. Rev.* E **60** 222
[6] Rodriguez-Plaza M J and Vazquez L 1990 *Phys. Rev.* B **41** 11 437
[7] Dziarmaga J and Zakrzewski W 1999 *Phys. Lett.* A **251** 8583
[8] Kamppeter T, Mertens F G, Sanchez A, Bishop A R, Dominguez-Adame F and Grønbech-Jensen N 1999 *Eur. Phys. J.* B **7** 607
[9] Kamppeter T, Mertens F G, Moro E, Sanchez A and Bishop A R 1999 *Phys. Rev.* B **59** 11 349
[10] Nakamura K and Sasada T 1974 *Phys. Lett.* A **48** 321
[11] Lakshmanan M, Ruijgrok T W and Thompson C J 1976 *Physica* A **84** 577
[12] Tjon J and Wright J 1977 *Phys. Rev.* B **15** 3470
[13] Fogedby H C 1980 *J. Phys. A: Math. Gen.* **13** 1467
[14] Roberts J A G and Thompson C J 1988 *J. Phys. A: Math. Gen.* **21** 1769
[15] Brown W F 1963 *Phys. Rev.* **130** 1677
[16] Iida S 1963 *J. Phys. Chem. Solids* **24** 625
[17] Garanin D A 1997 *Phys. Rev.* B **55** 3050
[18] Garcia-Palacios J L and Lazaro F J 1998 *Phys. Rev.* B **58** 14 937
[19] Garcia-Palacios J L 1999 unpublished
[20] Daniel M and Lakshmanan M 1983 *Physica* A **120** 125
[21] Gardiner C W 1983 *Handbook of Stochastic Methods for Physics, Chemistry and the Natural Sciences* (Berlin: Springer)
[22] San Miguel M and Toral R 1998 *Nonequilibrium Structures VI* ed E Tirapegui (Dordrecht: Kluwer)